

COMPUTATIONAL STUDY ON CONDUCTION HEAT TRANSFER THROUGH A THIN FILM GAUGE

A.R Abu Talib¹, P.T Ireland², A.J. Neely³, A.J Mullender⁴ and A.A Jaafar¹

¹Department of Aerospace Engineering, Universiti Putra Malaysia, 43400, Serdang, Selangor, Malaysia

²Department of Engineering Science, University of Oxford, OX1 3PJ Oxford, United Kingdom

³School of Aerospace, Civil & Mechanical Eng., University of New South Wales, ADFA, ACT 2600, Australia

⁴Rolls-Royce plc., Fire Precautions Group, P.O Box 31, Derby DE24 8BJ, United Kingdom

Email: abراهيم@eng.upm.edu.my

ABSTRACT

This paper presents a numerical analysis on conduction heat transfer through a custom built thin film gauge (TFG). The authors have developed a custom-built heat transfer gauge to measure the heat flux from ISO2685 fire-certification burner under isothermal wall conditions. During the calibration of TFG using a hot air gun, the heat flux from the hot air gun was not uniform. There was a high heat flux level directly underneath the hot plume. In order to investigate the effect of the non-uniform distribution of the heat flux, the author conducted a two-dimensional numerical analysis to confirm that one-dimensional conduction conditions prevailed throughout the temperature sensing section of the TFG. The numerical results were also compared directly to the temperature readings from the two thermocouples placed under the enamelled disc. The objective of this paper is to simulate the conduction heat transfer through the custom built TFG for fire-certification in aero engine. A detailed two-dimensional conduction analysis of the gauge is presented to assess the influence of lateral conduction on the gauge accuracy.

Keywords: thin film gauge, numerical analysis, heat transfer, fire-certification.

INTRODUCTION

Establish Heat Flux Measurement Techniques

ISO2685 [1] states that the heat flux from the standard burner must be calibrated using either a water-cooled copper tube calorimeter or an alternative, approved equipment. The specified calibration method requires a three minute warm-up time in order to obtain stable conditions before the temperature measurements are taken. During the test the temperature history of the constant flow of water is monitored every 30 seconds for a period of three minutes. The calibration procedure only provides a single measurement of heat flux averaged over the length of impingement of the flame onto the copper tube.

There are many methods of measuring heat flux such as those reported in Schultz and Jones [3], Jones [4] and Ainsworth et al. [5]. However, most of these methods were considered unsuitable for surveying the ISO2685 standard flame. A gauge for this purpose must be able to accurately measure a heat flux up to approximately 200 kW.m⁻² and be able to withstand prolonged immersion in a 2100°K flame. Thin film gauges (TFGs) were chosen to measure the surface temperature of an enamel insulating layer to a water-cooled metallic plate. As well as maintaining the gauges at manageable surface temperature, the water-cooled plate accurately prescribes the thermal boundary condition and avoids a large step in surface temperature between the gauge and its surroundings seen for uncooled surrounds [6]. Thin film gauges were selected to measure the surface temperature due to their fast response and ability to endure elevated surface temperatures.

Thin Film Gauge

Thin film gauge are widely used to measure transient and steady state heat transfer. Since 1970's the technique has been developed and used in a variety of gas turbine applications. Further application and development of the traditional TFG are described by Epstein [6], Doorly and Oldfield [8] and [9] and Dunn [10]. The development of the more recent direct heat transfer gauge is fully explained by Piccini [11] and Piccini et al. [12].

The TFG is used in conjunction with an insulating layer to measure surface temperature and local heat flux. In the steady state one-dimensional conduction, the magnitude of heat flux can be obtained from the solution of equation given as follows:

$$q = -\Delta T \left(\frac{k}{\Delta x} \right)$$

where k is the substrate thermal conductivity, Δx is the thickness of the insulator and ΔT is the temperature difference across the insulator. The temperature across a sheet, ΔT of a known thermal properties and dimensions is measured with the traditional platinum resistance sensor and a thermocouple is located on the rear face of the insulator.

The TFGs used in the current work consisted of five platinum films (approximately $0.04 \mu\text{m}$ thick) painted onto the surface of an enamelled Inconel disc (50 mm diameter and 2 mm thick), (Figure 1). Each platinum TFG is approximately 5 mm long and 1 mm wide. The enamel is assumed to have properties similar to fused quartz with thermal conductivity of $1.36 \text{ W.m}^{-1}.\text{K}^{-1}$ and a thickness of approximately $50 \mu\text{m}$ [13]. Inconel-600 (Nickel/Chromium alloy), which has a good oxidation resistance at high temperature and has a thermal conductivity of $14.8 \text{ W.m}^{-1}.\text{K}^{-1}$ at room temperature, was used as the base of the enamel. The gauges were connected using painted gold leads soldered to connecting wires.

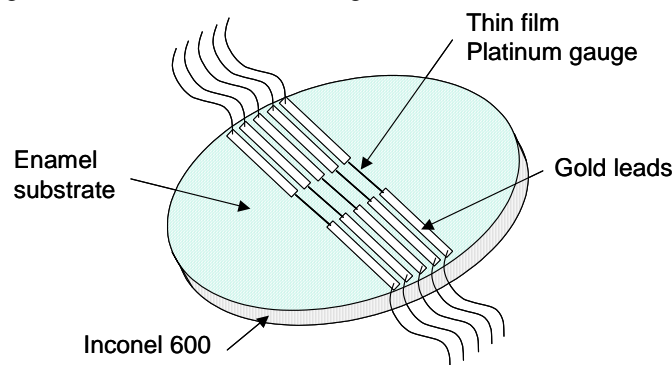


Figure 1: Enamelled Inconel disc painted with five platinum TFGs [6]

MATERIALS AND METHODS

During the calibration of TFG using the hot air gun, the heat flux from the hot air gun was not uniform. There was a high heat flux level directly underneath the hot plume. The flow field under the hot air gun is illustrated in Piccini [11]. In order to investigate the effect of the non-uniform distribution of the heat flux on the calibration, the author conducted a numerical prediction to confirm that one-dimensional conduction conditions prevailed throughout the temperature sensing section of the TFG. The numerical results were compared directly to the temperature readings from the two thermocouples placed under the enamelled disc as mentioned earlier in section (Figure 2). This enabled the author to simulate the low-temperature calibration procedure which involved the hot air gun.

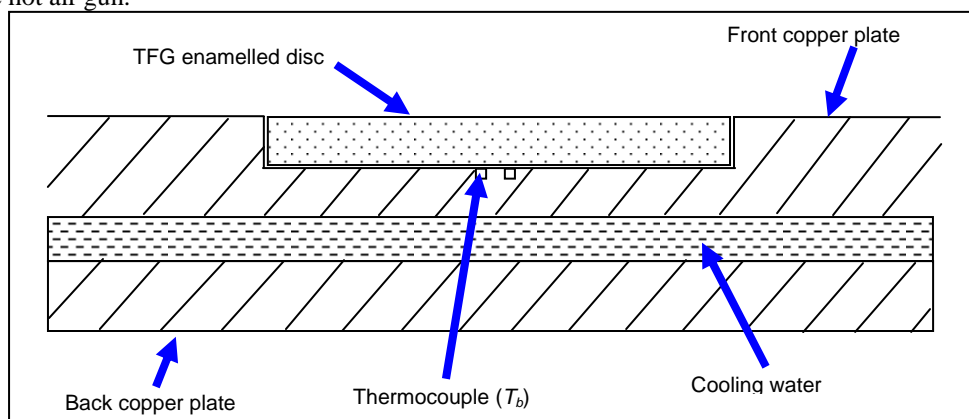


Figure 2: Schematic of the location of back surface thermocouple

The numerical method employed in this study is based on a finite-difference technique [14]. A finite difference method is used to discretised the transformed diffusion term in energy equation. Smaller spatial increments will result in reduce numerical errors but proportionately increase the number of equation to be solved. A uniform structured mesh in a physical domain (model of TFG) with 1 mm x 1 mm was formed. The system is considered as a two-dimensional body which is divided into equal increments in both x and y directions. The author used 1800 nodes to represent the whole system. The nodal points are designated as shown in Table 1(a), where the m locations indicate the x increment and n locations indicating the y increment. Laplace's equation is solved to determine the temperature at any of these nodal points. Assuming constant thermal conductivity and steady conditions with no heat generation, the temperature field must satisfy Laplace's equation given below;

$$\frac{\partial^2 T}{\partial x^2} + \frac{\partial^2 T}{\partial y^2} = 0 \quad (1)$$

The heat flow in the x and y directions may be calculated from the Fourier law of conduction;

$$q_x = -kA_x \frac{\partial T}{\partial x} \quad (2)$$

$$q_y = -kA_y \frac{\partial T}{\partial y} \quad (3)$$

Using Taylor's series approximation, the temperature gradients is discretised and neglecting the second order and higher term;

For x direction:

$$\left. \frac{\partial T}{\partial x} \right]_{(m+1)/2,n} \approx \frac{T_{m+1,n} - T_{m,n}}{\Delta x} \quad \text{and} \quad \left. \frac{\partial T}{\partial x} \right]_{(m-1)/2,n} \approx \frac{T_{m,n} - T_{m-1,n}}{\Delta x} \quad (4)$$

$$\left. \frac{\partial^2 T}{\partial x^2} \right]_{m,n} \approx \frac{\left. \frac{\partial T}{\partial x} \right]_{(m+1)/2,n} - \left. \frac{\partial T}{\partial x} \right]_{(m-1)/2,n}}{\Delta x} = \frac{T_{m+1,n} + T_{m-1,n} - 2T_{m,n}}{(\Delta x)^2} \quad (5)$$

For y direction:

$$\left. \frac{\partial T}{\partial y} \right]_{m,(n+1)/2} \approx \frac{T_{m,n+1} - T_{m,n}}{\Delta y} \quad \text{and} \quad \left. \frac{\partial T}{\partial y} \right]_{m,(n-1)/2} \approx \frac{T_{m,n} - T_{m,n-1}}{\Delta y} \quad (6)$$

$$\left. \frac{\partial^2 T}{\partial y^2} \right]_{m,n} \approx \frac{\left. \frac{\partial T}{\partial y} \right]_{m,(n+1)/2} - \left. \frac{\partial T}{\partial y} \right]_{m,(n-1)/2}}{\Delta y} = \frac{T_{m,n+1} + T_{m,n-1} - 2T_{m,n}}{(\Delta y)^2} \quad (7)$$

Thus the finite difference approximation for (1) becomes:

$$\frac{T_{m+1,n} + T_{m-1,n} - 2T_{m,n}}{(\Delta x)^2} + \frac{T_{m,n+1} + T_{m,n-1} - 2T_{m,n}}{(\Delta y)^2} = 0 \quad (8)$$

If $\Delta x = \Delta y$, then

$$T_{m+1,n} + T_{m,n+1} + T_{m-1,n} + T_{m,n-1} - 4T_{m,n} = 0 \quad (9)$$

The summary of the nodal equations for equal increments in x and y used throughout the analysis are displayed in Table 1.

Table 1: Summary of nodal formulae for finite-difference calculations [14]

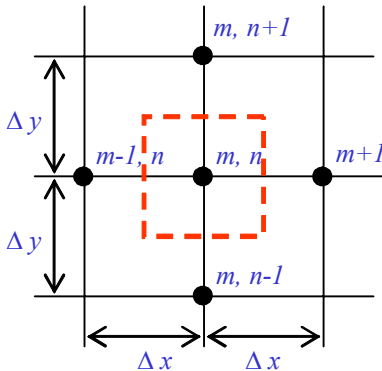
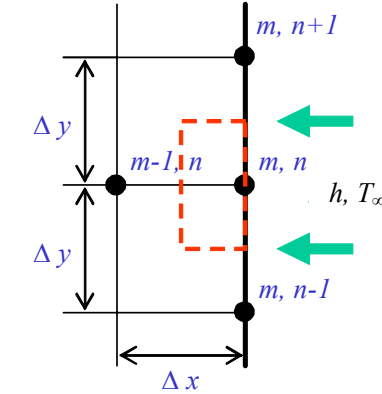
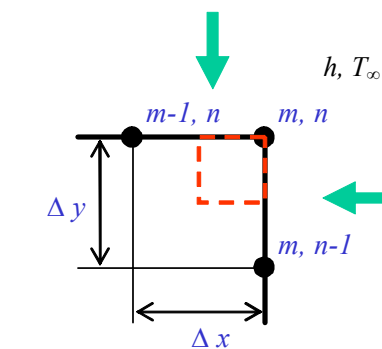
<p><u>a) Interior node</u></p> 	$0 = T_{m+1,n} + T_{m,n+1} + T_{m-1,n} + T_{m,n-1} - 4T_{m,n}$ $T_{m,n} = \frac{(T_{m+1,n} + T_{m,n+1} + T_{m-1,n} + T_{m,n-1})}{4}$
<p><u>b) Convection boundary node</u></p> 	$0 = \frac{h\Delta x}{k} T_{\infty} + \frac{1}{2}(2T_{m-1,n} + T_{m,n+1} + T_{m,n-1}) - \left(\frac{h\Delta x}{k} + 2\right) T_{m,n}$ $T_{m,n} = \frac{T_{m-1,n} + (T_{m,n+1} + T_{m,n-1})/2 + BiT_{\infty}}{2 + Bi}$ <p>Biot number, $Bi = \frac{h\Delta x}{k}$</p>
<p><u>c) Exterior corner with convection boundary</u></p> 	$0 = 2\frac{h\Delta x}{k} T_{\infty} + (T_{m-1,n} + T_{m,n-1}) - 2\left(\frac{h\Delta x}{k} + 1\right) T_{m,n}$ $T_{m,n} = \frac{(T_{m-1,n} + T_{m,n-1})/2 + BiT_{\infty}}{1 + Bi}$ <p>Biot number, $Bi = \frac{h\Delta x}{k}$</p>

Figure 3 shows a two dimensional physical representation of the enamelled inconel disc and copper plate (300 mm x 6 mm). The algebraic is written at each node depending on the position of the node in the system according to Table 1. Since the aim of this analysis was to assess the influence of heat conduction in the x direction on the gauge calibration, the numerical model did not include the thin enamel insulator on the front surface of the inconel disc. The heat flux (q) and freestream temperature (T_{∞}) data from the heat flux calibration of TFG were used as the boundary conditions for the computation. The variable hot air gun was set to produce a hot air flow of 100°C. It was assumed that T_{∞} from the hot air gun was uniform across the area of the inconel disc. The ambient temperature (T_o) was 293°K and the water temperature (T_{water}) was 283°K. The thermal conductivity (k) of copper and inconel are assumed to be uniform at 386 W.m⁻¹.K⁻¹ and 14.8 W.m⁻¹.K⁻¹

respectively. The system of algebraic equation solved iteratively using Gaussidel method on Microsoft Excel and simulated the temperature distribution over the full copper plate. T_o and T_b are the ambient surrounding temperature and back temperature respectively. T_b is taken from the water temperature at equilibrium conditions.

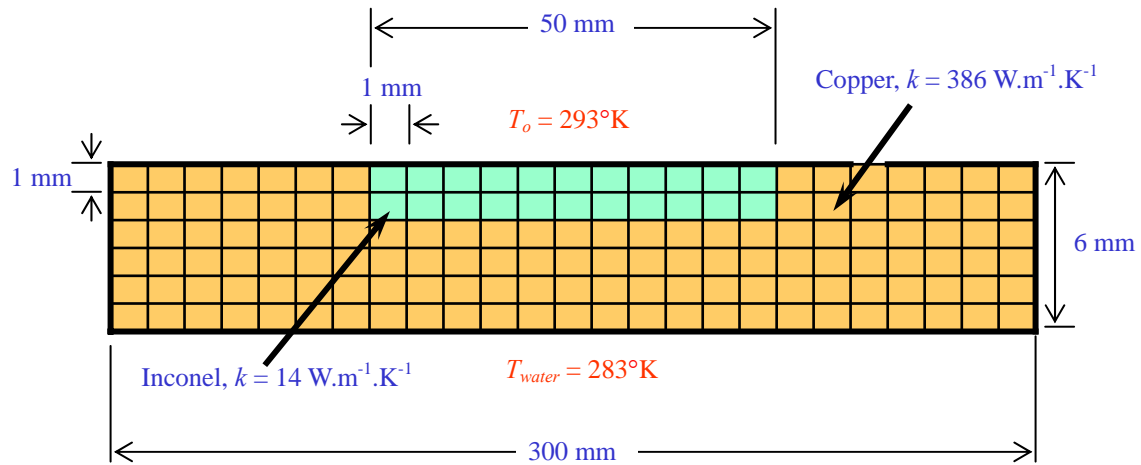


Figure 3: Two-dimensional physical presentation of the enamelled inconel disc and copper plate

RESULTS AND DISCUSSION

The distributions of q from the heat flux calibration using the hot air gun are shown in Figure 4.

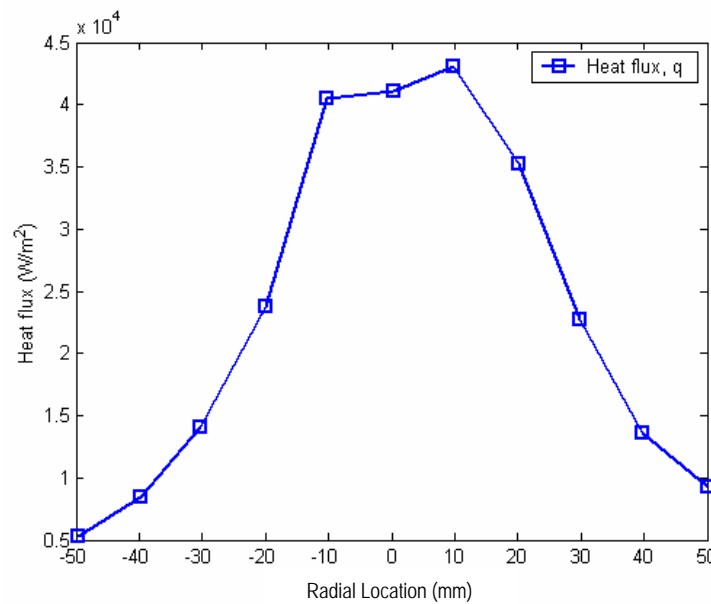


Figure 4: Distribution of heat flux (q) from the TFG heat flux calibration using a hot air gun

Figure 5 shows a plot of temperature against radial location for various depths in the plate. The computational data were then compared to data (T_{back}) from thermocouples placed underneath the inconel disc. It was found that the numerical prediction on the temperature levels at 2 mm depth (shown in red line in Figure 5) were near to the values measured from the back thermocouple during the calibration. This allowed more confidence in the temperature readings obtained from the back thermocouple. Figure 6 shows the temperature gradient along the vertical centreline. The computational result showed that the heat flow is dominant in one direction and the lateral heat conduction is significantly small. The full temperature distribution in the plate is shown in Figure 7. It can be summarised that there is a uniform temperature distribution of heat penetration inside the inconel disc and copper plate during both the calibration processes.

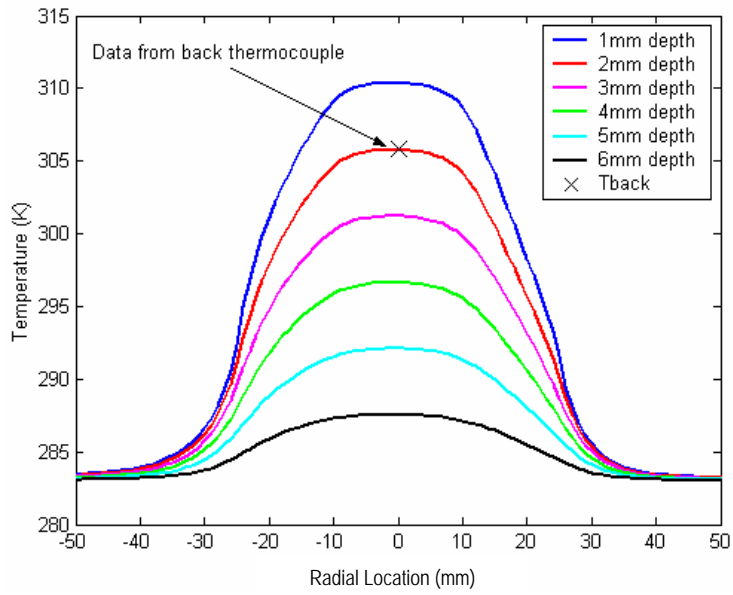


Figure 5: Numerical analysis result from TFG hot air gun calibration

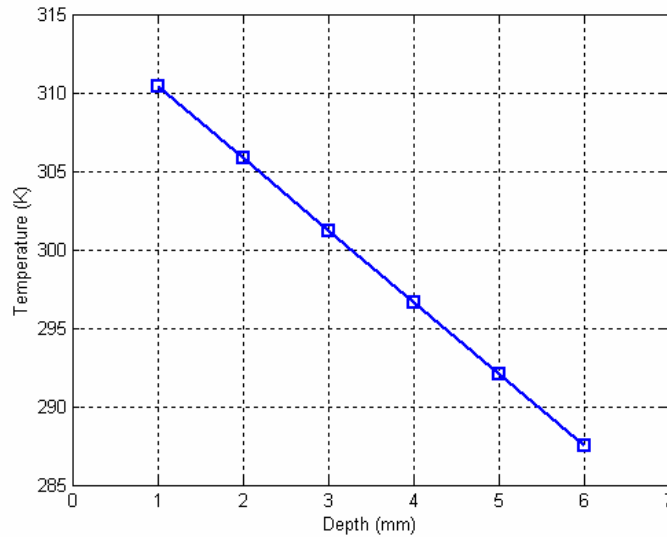


Figure 6: Plot of temperature against depth at the centre of the inconel disc

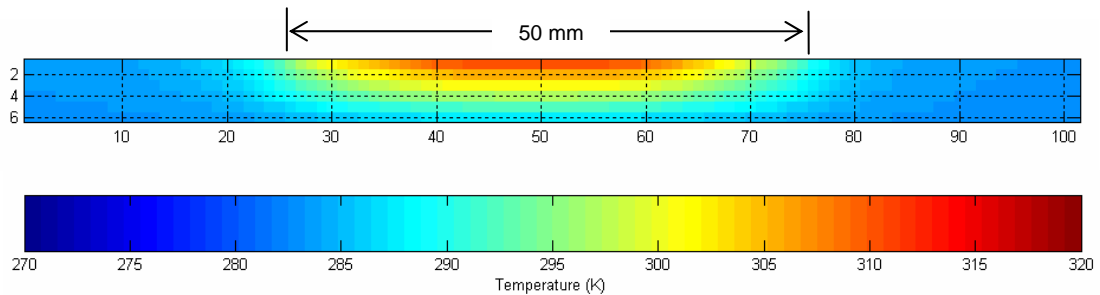


Figure 7: Temperature distribution from numerical analysis of the TFG hot air gun calibration the effect of different hydrogen flow rates.

CONCLUSION

A detailed two-dimensional conduction analysis on the custom built thin film gauge was successfully conducted. The results obtained from the prediction confirmed that the temperature distribution in the plate was essentially one-dimensional during the thin film gauge calibration of TFG using hot air gun. The contribution of lateral conduction on the uncertainty of the TFG is considered small.

ACKNOWLEDGEMENT

The authors wish to thank the UK Ministry of Defence (MoD) and the UK Department of Trade and Industry (DTI) for their financial support for this work through the Defence Evaluation and Research Agency (DERA), Pyestock. The first author thanks the Malaysian Government and the University Putra Malaysia for their financial support.

REFERENCES

- [1] The International Organisation for Standardisation (1992) Aircraft - Environmental Conditions and Test Procedures for Airborne Equipment - Resistance to Fire in Designated Fire Zones, ISO2685:1992(E).
- [2] Wright, G. (2000) Fire Certification in Aero Engines, 4th Year Project Report, Department of Engineering Science, University of Oxford, Oxford, UK.
- [3] Schultz, D.L. and Jones, T.V. (1973) Heat Transfer Measurements in Short Duration Hypersonic Facilities, AGARD-AG-165, Advisory Group for Aerospace Research & Development (AGARD).
- [4] Jones, T.V. (1977) Heat Transfer, Skin Friction, Total Temperature and Concentration Measurements, Measurement of Unsteady Fluid Dynamic Phenomena, von Karman Institute for Fluid Dynamics.
- [5] Ainsworth, R.W., Allen, J.L., Davies, M.R., Forth, C.J.P., Hilditch, M.A., Oldfield, M.L.G. and Sheard, A.G. (1989) Developments in Instrumentation and Processing for Transient Heat Transfer Measurements in a Full-stage Model Turbine, Transactions of the ASME Journal of Turbomachinery, **111**: 20-27.
- [6] Abu Talib, A.R., Neely, A.J., Ireland, P.T. and Mullender, A.J. (2005) Detailed Investigation of Heat Flux Measurements Made in a Standard Propane-Air Fire-Certification Burner Compared to Levels Derived From a Low-Temperature Analogue Burner, Journal of Engineering for Power and Gas Turbines, **127**(2): 249-256.
- [7] Epstein, A.H., Guenette, G.R., Norton, R.J.G. and Yuzhan, G. (1986) "High Frequency Response Heat Flux Gauges, Review Scientific Instrument, **57**(4): 639-649.
- [8] Doorly, J.E. and Oldfield, M.L.G. (1986) New Heat Transfer Gauges for Use on Multilayered Substrates, Transactions of the ASME Journal of Turbomachinery, **108**: 153-160.
- [9] Doorly, J.E. and Oldfield, M.L.G. (1987) The Theory of Advanced Heat Transfer Gauges, International Journal of Heat Transfer, **30**(6): 1159-1168.
- [10] Dunn, M. G. (1989) Phase and Time Resolved Measurements of Heat Transfer and Pressure in a Full Stage Rotating Turbine, Proceedings, ASME/IGTi Turbo Expo, 89-GT-135.
- [11] Piccini, E., (1999) The Development of a New Heat Transfer Gauge for Heat Transfer Facilities, MSc Thesis, Department of Engineering Science University of Oxford, Oxford, UK.
- [12] Piccini, E., Guo, S.M. and Jones, T.V. (2000) The Development of a New Direct-Heat-Flux Gauge for Heat-Transfer Facilities, Measurement Science Technology, **11**: 342-349.
- [13] Doorly, J.E. (1985) The Development of Heat Transfer Measurement Technique for Application to Rotating Turbine Blades, D.Phil Thesis, Department of Engineering Science University of Oxford, Oxford, UK.
- [14] Holman, J.P. (1997) Heat Transfer, McGraw-Hill. 8th International Edition.

NOMENCLATURE

A	surface area	(m ²)	T	temperature	(K)
Bi	Biot number, $Bi = \frac{h\Delta x}{k}$		T_{∞}	freestream temperature	(K)
h	heat transfer coefficient	(W.m ⁻² .K ⁻¹)	T_0	ambient temperature	(K)
k	thermal conductivity	(W.m ⁻¹ .K ⁻¹)	T_b	back temperature	(K)
m	x direction increment		T_{water}	water temperature	(K)
n	y direction increment		ΔT	temperature difference	(K)
q	heat flux or heat load	(W.m ⁻²)	Δx	thickness of the insulator	(m)